THE JOURNAL OF PHYSICAL CHEMISTRY A

Article

pubs.acs.org/JPCA

Vacuum-Ultraviolet Electronic Circular Dichroism Study of Methyl α-D-Glucopyranoside in Aqueous Solution by Time-Dependent Density Functional Theory

Koichi Matsuo,*[,†] Hirofumi Namatame,[†] Masaki Taniguchi,[†,‡] and Kunihiko Gekko[§]

[†]Hiroshima Synchrotron Radiation Center, Hiroshima University, Higashi-Hiroshima 739-0046, Japan

[‡]Department of Physical Science, Graduate School of Science, Hiroshima University, Higashi-Hiroshima 739-8526, Japan

[§]Institute for Sustainable Sciences and Development, Hiroshima University, Higashi-Hiroshima 739-8526, Japan

Supporting Information

ABSTRACT: The vacuum-ultraviolet (VUV) electronic circular dichroism (ECD) spectrum of methyl α-D-glucopyranoside (methyl α-D-Glc) was measured down to 163 nm in aqueous solution using a synchrotron-radiation VUV-ECD spectrophotometer. The spectrum exhibited two characteristic ECD peaks around 170 nm, which depend on the trans (T) and gauche (G) configurations of the hydroxymethyl group at C-5. To elucidate the influences of the T and G configurations on the spectrum, the ECD spectra of three rotamers (α-GT, α-GG, and α-TG) of methyl α-D-Glc were calculated using time-dependent density functional theory (TDDFT) combined with molecular dynamics simulation. A linear combination of the ECD spectra of these three rotamers, which differ markedly from each other, produced a methyl α-D-Glc spectrum similar to that observed experimentally. The spectrum was assignable to the $n-\sigma^*$ transitions of the ring oxygen and methoxy oxygen with minor contributions from the hydroxyl oxygen. The differences in α-GT, α-GG, and α-TG spectra were attributed to fluctuations of the configurations of the hydroxymethyl group at C-5 and the hydroxyl group at C-4, which strongly affected the orientations of intramolecular hydrogen bonds around the ring oxygen. These findings demonstrate that combining VUV-ECD and TDDFT is useful for structural characterization of saccharides in aqueous solution.

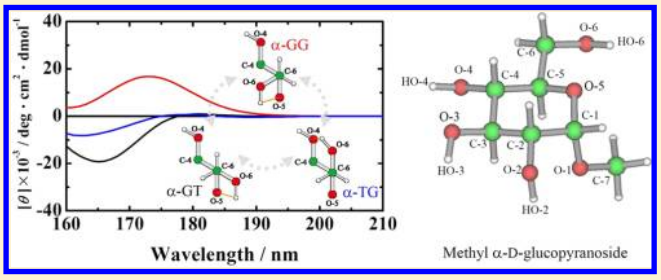

1. INTRODUCTION

Vacuum-ultraviolet (VUV) electronic circular dichroism (ECD) spectroscopy is a powerful technique for the structural analysis of biomolecules, including saccharides.[1−3] This technique is highly advantageous for unsubstituted saccharides because they contain hydroxyl groups and acetal bonds whose high-energy $n-\sigma^*$ transitions are detectable only below 190 nm.[4−7] The VUV-ECD spectra of monosaccharides and methyl aldopyranosides were first measured down to ∼165 nm in aqueous solution by Johnson and his co-workers.[4,5,8] They found that the gauche (G) and trans (T) configurations of the hydroxymethyl group at C-5 and the axial and equatorial configurations of the hydroxyl groups at C-2 and C-4 are decisive factors for the VUV-ECD spectra of these saccharides. Arndt and Stevens also measured the VUV-ECD spectra of α- and β-methyl aldopyranosides down to ∼140 nm in films, and decomposed them into four types of $n-\sigma^*$ electronic transitions mainly due to the ring oxygen in the wavelength region from 150 to 190 nm.[6] Matsuo and Gekko measured the VUV-ECD spectra of five monosaccharides down to 160 nm in aqueous solution using a synchrotron-radiation VUV-ECD spectrophotometer,[9−11] and predicted the six component spectra of the α-GT, α-GG, α-TG, β-GT, β-GG, and β-TG conformers by deconvolution analyses based on a Gaussian distribution.[7] Despite these steady efforts, however, the principle of pairwise relationships between the configurations and the ECD spectra of monosaccharides remain unclear, because the conformations of monosaccharides are in equilibrium between the α- and β-anomers and between the G and T configurations in aqueous solution, and several electronic transitions of the hydroxyl group and acetal bond coexist in the wavelength region from 190 to 140 nm.[6−8]

Ab initio calculations and molecular dynamics (MD) simulations have been applied for analyzing such complicated conformations of monosaccharides in aqueous solution.[12−17] Momany and his co-workers optimized several structures of GT, GG, and TG rotamers of α- and β-glucopyranoses by density functional theory (DFT) and showed that the theoretical α/β anomeric ratio of D-glucose (∼32/68) is in agreement with the experimental value (∼36/64).[14,15] Moreover, MD simulations of saccharides such as α- and β-glucopyranoses in aqueous solution revealed the characteristic configurations of hydroxymethyl and hydroxyl groups restricted by the hydrogen bonds with water molecules,[16−19] and the

Received: July 12, 2012
Revised: September 5, 2012
Published: September 5, 2012

numbers of water molecules hydrated to glucose.[20−23] These results demonstrate that ab initio calculations and MD simulations are useful for analyzing the configurations of hydroxymethyl and hydroxyl groups of monosaccharides in aqueous solution. On the other hand, a time-dependent DFT (TDDFT) method has been successfully used to calculate the ECD spectra of small biomolecules. Fukuyama et al. found that the ECD spectra of L-alanine and L-lactic acid calculated using the TDDFT method with nine- and six-hydrated water molecules, respectively, were close to those observed experimentally.[24,25] Šebek et al. compared the VUV-ECD spectra of dialanine down to 170 nm at pH values of 1.43, 6.17, and 12.1 with those calculated using the TDDFT method, and concluded that the anionic, cationic, and zwitterionic forms of dialanine were hydrated with 10 water molecules.[26] Nielsen et al. calculated the ECD spectra of adenine and thymine to investigate the fingerprints of bonding motifs in DNA duplexes.[27] These observations indicate that theoretical analyses of ECD using the DFT, MD, and TDDFT methods would give new information about the complicated equilibrium structures and the assignments of ECD spectra of monosaccharides in aqueous solution.

In the present study, to elucidate the influences of T and G configurations of the hydroxymethyl group on the ECD spectra of monosaccharides, we measured the VUV-ECD spectrum of methyl α-D-glucopyranoside (methyl α-D-Glc) and compared it with the spectrum calculated theoretically using the DFT, MD, and TDDFT methods. The contributions of the hydroxymethyl group, hydroxyl groups, and the ring oxygen to the VUV-ECD spectrum are discussed in terms of the hydration and intramolecular hydrogen bonds, which are decisive factors for the α-GT, α-GG, and α-TG conformations of the hydroxymethyl group (see Figure 1). This is the first time that TDDFT has been applied to the theoretical analysis of VUV-ECD of saccharides in aqueous solution.

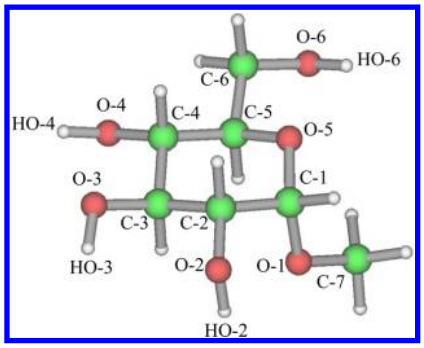

Figure 1. Crystal structure of the α-GT rotamer of methyl α-D-Glc. Oxygen, hydrogen, and carbon atoms are colored red, white, and green, respectively. The dihedral angles of O-5−C-5−C-6−O-6 involving the hydroxymethyl group at C-5 are 60, −60, and 180° for the α-GT, α-GG, and α-TG rotamers, respectively.

2. MATERIALS AND METHODS

2.1. Materials. Methyl α-D-Glc of high purity (>98%) was purchased from Sigma-Aldrich (St. Louis, MO) and used without further purification. Methyl α-D-Glc solution was freshly prepared by dissolving in heavy water at a concentration of 10.0 (w/v %). The concentration of the solute was determined by a dry-weight method. The obtained sample solution was incubated at room temperature for 1 day before performing VUV-ECD measurement.

2.2. VUV-ECD Measurement. The VUV-ECD spectrum of methyl α-D-Glc was measured in the wavelength region from 210 to 163 nm at 25 °C using a VUV-ECD spectrophotometer at Hiroshima Synchrotron Radiation Center. The details of the optical devices of the spectrophotometer are available elsewhere.[9,10] The VUV-ECD measurement was carried out using an assembled-type optical cell with CaF_2 windows.[10] The path length of the cell was adjusted with a Teflon spacer to 10 μm for the measurements down to 172 nm, and no spacer was used for the measurements below 172 nm to reduce the effects of light absorption by the solvent. The spectra obtained without the spacer were calibrated by normalizing the ellipticities to the spectra measured using a 10 μm spacer in the overlapping wavelength region from 210 to 172 nm. The path length of the cell without spacer was estimated to be 1.4 μm by this calibration method. The spectrum was recorded with a 1.0 mm slit, an 8 s time constant, and an 8 nm/min scan speed and using four accumulations. The molar ellipticity, $[\theta]$, was calculated using the molecular weight of the solute. The ellipticity was reproducible within an error of ±5%, which was mainly attributable to noise and to inaccuracy in the light path length.

2.3. Initial Structures. The GT crystal structure of methyl α-D-Glc[28] (Figure 1) was adopted as the initial structure of the α-GT rotamer. The initial structures of the α-GG and α-TG rotamers were constructed by exchanging the positions of the hydroxyl group and the hydrogen atom at C-6 in the α-GT crystal structure (see Figure 1).

2.4. Optimization. A DFT method at the B3LYP level has been successfully applied for optimizing the structures of small biomolecules in aqueous solution.[12−14,24−26] Further, the Coulomb-attenuated method B3LYP (CAM-B3LYP) that combines the B3LYP with long-range correction was recently developed to improve the description of the charge-transfer excited states and the weak interactions.[29,30] Hence, the present study used the CAM-B3LYP method for optimizing the geometry of the α-GG, α-GT, and α-TG rotamers. The preliminary geometry optimizations were carried out at the CAM-B3LYP/6-31+G* level, followed by optimizations at the CAM-B3LYP/6-311++G** level. The effects of the solvent on the structures of solutes were taken account using a continuum model with the dielectric constant of water (78.39) and the recommended cavity radius for a solute volume. Optimization was performed with the Gaussian 09 program[31] on an HPC 3000 computer (HPC Systems, Japan).

2.5. Molecular Dynamics Simulations. The initial structures of the α-GG, α-GT, and α-TG rotamers were loaded into the xLEaP software in AMBER 11[32] and immersed in a periodic box (with approximate dimensions of 28 Å × 28 Å × 25 Å) with 650 TIP3P water molecules.[33] Each initial structure was energy-minimized and simulated under the AMBER/GLYCAM force field[34] as follows. Initial steepest-descent energy minimization (1000 cycles) was performed on the system to relax any steric hindrances artificially produced by the initialization procedure. The energy minimization was carried out for 200 ps while increasing the temperature of the system from 0 to 298 K. After heating, the obtained system was simulated for 20 ns at 298 K and 1 atm using the Berendsen coupling algorithm[35] with τ = 1.0 ps. The particle-mesh Ewald method[36] was used for calculating the electrostatic interactions, with a cutoff of 8 Å for the direct-space sum. We also used a

cutoff of 8 Å for the van der Waals interactions. The SHAKE algorithm with an integration time step of 1.0 fs[37] was applied to constrain all of the bonds involving hydrogen. To suppress switching among α-GG, α-GT, and α-TG conformations, the dihedral angle of O-5−C-5−C-6−O-6 was slightly constrained to any of the three conformations using the "RESTRAINT-MASK" keyword.[38]

2.6. Calculation of ECD Spectra. ECD is induced by the interaction between electric and magnetic dipole transition moments of chromophores and the electromagnetic field of a light wave. As for the relationship between absorption and the dipole strength, ECD is related to the rotational strength, R, which is theoretically defined by[2,24]

$$R_{0a} = \mathrm{Im}\{\langle\Psi_0|\hat{\boldsymbol{\mu}}|\Psi_a\rangle\cdot\langle\Psi_a|\hat{\mathbf{m}}|\Psi_0\rangle\} \quad (1)$$

where R_{0a} is the rotational strength of the electric transition from the "0" to "a" state, $\hat{\boldsymbol{\mu}}$ and $\hat{\mathbf{m}}$ are the electric and magnetic dipole moments, respectively, and Im{} indicates the imaginary part of a complex number. The rotational strength is expressed in cgs units (erg cm^3), which are conveniently transformed into Debye-Bohr magnetons (DBM) according to 1 DBM = 0.9273 × 10^{-38} erg cm^3 = 0.9273 × 10^{-51} J m^3.

The final ECD spectrum can be calculated using the following equations:

$$R_i = 1.23 \times 10^{-42}\frac{[\theta]_i \Delta\sigma}{\sigma_i} \quad (2)$$

$$[\theta](\sigma) = \sum_i [\theta]_i \exp\left[-\left(\frac{\sigma-\sigma_i}{\Delta\sigma}\right)^2\right] \quad (3)$$

where $[\theta]$ is the molar ellipticity, σ_i is the energy of the ith transition, and $\Delta\sigma$ is the half bandwidth of a spectrum calculated assuming a Gaussian distribution. The ECD spectra were calculated using the Gaussian 09 program. The rotational strength, R_i, was calculated using a TDDFT method at the CAM-B3LYP/6-311++G** level and a polarized continuum model[39] to account for the effects of the solvent. From the obtained rotational strength, ECD spectra were calculated using eqs 2 and 3 with a $\Delta\sigma$ value of 0.40 eV. All theoretical spectra were calculated in the energy scale and converted to the wavelength scale. Thirty excited states were considered for the TDDFT calculations.

3. RESULTS AND DISCUSSION

3.1. VUV-ECD Spectrum of Methyl α-D-Glucopyranoside. Figure 2 shows the VUV-ECD spectrum of methyl α-D-Glc in heavy water down to 163 nm, which was obtainable by reducing light absorption by the solvent. The observed spectrum, which has a positive peak around 172 nm and a negative peak around 164 nm, was very close to that measured in water by Nelson and Johnson,[5] indicating that the spectrum in heavy water can be essentially discussed as in light water. On the other hand, the VUV-ECD of methyl α-D-Glc in film exhibited a positive peak around 170 nm and a negative peak around 160 nm,[6] which were slightly different from those in water probably due to different populations of the α-GG, α-GT, and α-TG rotamers[4,5,7,8] and/or different electronic states of chromophores in the solution and solid states. These results demonstrate that the solvent water is an indispensable factor in simulating the structures and VUV-ECD spectra of monosaccharides in solution.

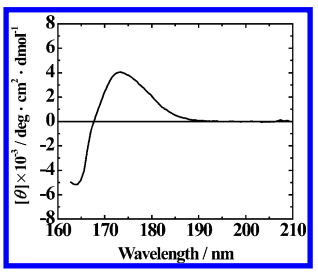

Figure 2. Experimentally observed VUV-ECD spectrum of methyl α-D-Glc in aqueous solution. The spectrum was recorded with a 1.0 mm slit, an 8 s time constant, and an 8 nm/min scan speed and using four accumulations.

3.2. Optimized Structures and ECD Spectra of Methyl α-D-Glucopyranoside in Water (Onsager Model). The structures of the α-GT, α-GG, and α-TG rotamers were optimized in water (Onsager model) using the DFT method at the CAM-B3LYP/6-311++G** level and their molecular parameters (bond lengths, bond angles, and dihedral angles) listed in Table 1. The structural differences among the α-GT, α-GG, and α-TG rotamers are prominently indicated by their O-5−C-5−C-6−O-6 dihedral angles being 60.2, −61.5, and 176.3°, respectively. In addition, some definite differences can be observed in the dihedral angles involving hydroxyl groups; that is, HO-2−O-2−C-3−C-1, HO-4−O-4−C-4−C-3, and HO-6−O-6−C-6−C-5 (Table 1). For example, the HO-4−O-4−C-4−C-3 dihedral angles are −45.7 and 77.4° for the α-GG and α-TG rotamers, respectively, and those of HO-6−O-6−C-6−C-5 are −56.1 and 35.6° for the α-GT and α-TG rotamers, respectively. Similar structural differences among the three rotamers were also observed in the optimized structures of D-glucopyranose with five hydrated water molecules.[14]

The ECD spectra of the α-GT, α-GG, and α-TG rotamers were calculated with their optimized structures using the TDDFT method at the CAM-B3LYP/6-311++G** level, and the ECD spectrum of methyl α-D-Glc was estimated by a linear combination of the spectra of the three rotamers based on their relative populations (α-GT:α-GG:α-TG = 38:58:4).[40] The obtained ECD spectra are shown in Figure 3. The α-GT, α-GG and α-TG rotamers exhibit characteristic peak positions and intensities below 190 nm: α-GT and α-GG rotamers exhibit a negative peak around 175 nm and a positive peak around 165 nm but with markedly different intensities, whereas the α-TG rotamer shows a positive peak around 165 nm with an indistinct shoulder around 175 nm. These differences in spectra may be mainly due to the dihedral angles involving the hydroxymethyl and hydroxyl groups as described above. The estimated spectrum of methyl α-D-Glc is evidently very different from that observed experimentally (Figure 2), in terms of a negative peak around 175 nm and a positive peak around 165 nm. This inconsistency indicates a limitation of the Onsager model for evaluating the effects of the solvent with a continuum model, and that a detailed MD simulation is required for the structures of the three rotamers including the hydrated water molecules.

3.3. Molecular Dynamics Simulations of Methyl α-D-Glucopyranoside in a Water Bath. The number of hydrated water molecules of D-glucose has been experimentally estimated to be 10, 8.4, 3.3, 2.3, and 2.2 by IR spectroscopy,[41,42] density and ultrasound measurements,[43] compressibility,[44] dielectric relaxation,[45] and NMR measurements,[45] respectively. Some theoretical studies[14,24−27] assumed that the structures of small

Table 1. Bond Lengths, Bond Angles, and Dihedral Angles of the Optimized and Simulated Structures of the α-GT, α-GG, and α-TG Rotamers

	α-GT			α-GT			α-GT		
		MD			MD			MD	
	Onsager model	10 ns	20 ns	Onsager model	10 ns	20 ns	Onsager model	10 ns	20 ns
				Bond Length (Å)					
O-5−C-5	1.446	1.421	1.498	1.443	1.446	1.430	1.434	1.430	1.468
C-1−O-5	1.461	1.424	1.447	1.450	1.403	1.378	1.423	1.493	1.467
O-1−C-1	1.406	1.539	1.504	1.384	1.370	1.482	1.406	1.485	1.485
C-6−C-5	1.521	1.546	1.516	1.523	1.492	1.475	1.530	1.582	1.508
C-3−C-4	1.523	1.490	1.514	1.531	1.539	1.551	1.530	1.580	1.526
C-7−O-1	1.429	1.485	1.447	1.435	1.412	1.419	1.442	1.486	1.524
				Bond Angle (deg)					
C-1−O-5−C-5	115.933	116.170	112.840	112.810	115.920	121.520	116.313	115.030	119.430
O-1−C-1−O-5	113.303	109.765	109.725	111.676	108.347	112.711	112.730	113.434	105.670
C-7−O-1−C-1	114.905	110.590	108.290	114.890	114.230	118.000	114.252	109.220	116.800
O-5−C-5−C-4	109.617	111.240	104.220	107.570	110.250	107.190	109.165	109.350	108.670
O-5−C-5−C-6	105.790	102.110	107.022	109.930	105.500	104.560	106.126	100.410	107.150
HO-6−O-6−C-6	107.021	118.540	108.020	109.910	105.510	113.350	106.528	110.570	111.230
C-1−C-2−C-3	110.429	114.037	110.089	109.716	113.515	108.988	109.612	111.130	113.066
				Dihedral Angle (deg)					
C-7−O-1−C-1−O-5	71.2727	68.079	69.018	82.024	68.399	59.901	71.105	68.788	88.353
HO-2−O-2−C-2−C-1	−43.587	43.260	98.551	156.238	63.699	−57.337	−7.993	−58.315	−52.265
HO-4−O-4−C-4−C-3	46.838	86.550	65.017	−45.666	−44.366	138.776	77.442	84.543	69.415
C-1−O-5−C-5−C-4	58.750	69.170	69.320	66.030	63.440	56.360	57.744	63.120	46.360
O-5−C-5−C-4−C-3	−56.706	−61.090	−62.380	−60.760	−58.250	−42.980	−57.868	−49.700	−45.800
C-5−C-4−C-3−C-2	56.214	53.640	55.460	56.810	53.338	49.060	59.396	43.550	47.470
O-5−C-5−C-6−O-6	60.2185	59.830	77.550	−61.490	−53.670	−64.420	176.256	−179.460	179.590
HO-6−O-6−C-6−C-5	−56.090	−79.360	−71.590	93.090	51.320	64.900	35.593	39.610	23.410

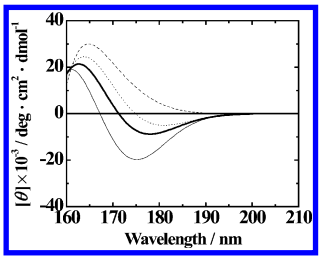

Figure 3. Theoretical ECD spectra of the α-GT (thin solid line), α-GG (dotted line), and α-TG (dashed line) rotamers of methyl α-D-Glc calculated using the Onsager model by the TDDFT method at the CAM-B3LYP/6-311++G** level. The thick solid line shows the ECD spectrum of methyl α-D-Glc estimated by a linear combination of the α-GT, α-GG, and α-TG spectra based on their relative populations (α-GT:α-GG:α-TG = 38:58:4).[40]

biomolecules, including methyl α-D-Glc, are reproducible with several hydrated water molecules. However, Simmerling et al. showed that the dihedral angles involving hydroxyl groups and the sugar ring of glucose fluctuate in a water bath during MD simulations.[16] These fluctuations in the water bath were also observed for the dihedral angles involving glycoside bonds of trehalose, maltose, and sucrose.[22,23] Therefore, we simulated the structures of methyl α-D-Glc in a water bath without fixing the number of hydrated water molecules.

The structures of three rotamers (α-GT, α-GG, and α-TG) of methyl α-D-Glc were simulated in a water bath for 20 ns using AMBER 11 software (see the Materials and Methods). The dihedral angles of O-5−C-5−C-6−O-6 (60° for α-GT, −60° for α-GG, and 180° for α-TG) were slightly restricted by the "RESTRAINTMASK" command to within similar distribution ranges (about ±30°) as those of glucose obtained without restriction.[16,17] The molecular parameters of the simulated α-GT, α-GG, and α-TG rotamers at 10 and 20 ns are compared in Table 1 with those of the optimized structures obtained using the Onsager model. The bond lengths and bond angles of each rotamer are almost invariable in the MD-simulated and Onsager-optimized structures, but there are large differences in the dihedral angles involving the methoxy group (C-7−O-1−C-1−O-5), hydroxymethyl group (O-5−C-5−C-6−O-6), and hydroxyl groups (e.g., HO-4−O-4−C-4−C-3). We examined the fluctuations of these groups by plotting the dihedral angles involving the methoxy group (C-7−O-1−C-1−O-5) and hydroxyl group (HO-4−O-4−C-4−C-3) of the α-GT rotamer against simulation time up to 20 ns. As shown in Figure 4a, the dihedral angle of C-7−O-1−C-1−O-5 converged to 75 ± 30°, but that of HO-4−O-4−C-4−C-3 showed a wide variation: two stable configurations seem to exist around −60 and 150° in addition to a dominant population around 60°. Similar fluctuations in the dihedral angle of HO-4−O-4−C-4−C-3 were also observed for the α-GG and α-TG rotamers (Figures S1a and S2a, Supporting Information, and Table 1).

Table 2 lists the mean numbers of water molecules that exhibit hydrogen bonding (with a H−O_A distance ≤2.4 Å and an O_D−H−O_A angle >120°, where O_D and O_A are the donor and acceptor oxygens, respectively)[19,21] to the hydroxyl groups at C-6, C-4, C-3, and C-2, the ring oxygen (O-5), and the methoxy oxygen (O-1) in the α-GT, α-GG, and α-TG rotamers. In this table, the total numbers of water molecules (10.1−10.6) are smaller than the sum of the numbers for four hydroxyl groups (2.1−2.8), the ring oxygen (0.6−0.9), and the methoxy oxygen (1.0−1.2), which is due to a water molecule—being both a hydrogen donor and acceptor—having the

dx.doi.org/10.1021/jp306914s | J. Phys. Chem. A 2012, 116, 9996−10003

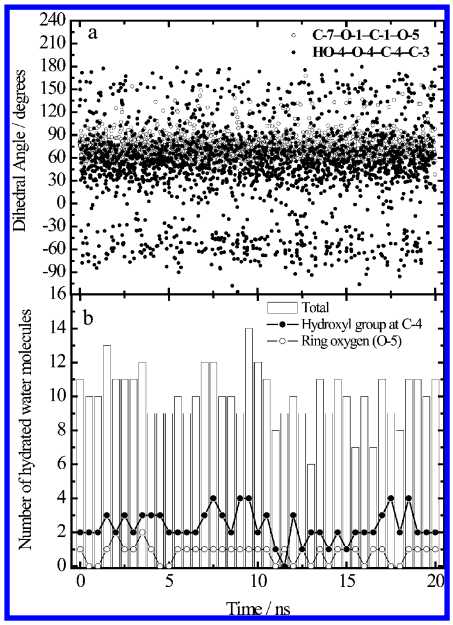

Figure 4. Configuration changes of the α-GT rotamer during the simulation as monitored by (a) the dihedral angles of the methoxy group (C-7−O-1−C-1−O-5) and the hydroxyl group (HO-4−O-4−C-4−C-3) and (b) the numbers of water molecules exhibiting hydrogen bonding to the α-GT molecule (total), the hydroxyl group at C-4, and the ring oxygen (O-5). The dihedral angles and the numbers of hydrated water molecules were determined at 10 and 500 ps intervals, respectively.

Table 2. Mean Numbers of Water Molecules That Exhibit Hydrogen Bonding to the Hydroxyl Groups at C-6, C-4, C-3, and C-2, the Ring Oxygen (O-5), and the Methoxy Oxygen (O-1) in the Simulated Structures of the α-GT, α-GG, and α-TG Rotamers

		hydroxyl groups at				ring oxygen	methoxy oxygen
	total	C-6	C-4	C-3	C-2	O-5	O-1
α-GT	10.1	2.8	2.4	2.3	2.7	0.9	1.1
α-GG	10.6	2.8	2.4	2.4	2.8	0.6	1.0
α-TG	10.4	2.4	2.1	2.6	2.7	0.7	1.2

potential to form two hydrogen bonds with an oxygen atom and a hydroxyl group. These numbers of water molecules for the rotamers of methyl α-D-Glc are very close to those for D-glucose estimated by MD simulations, in terms of the total number (~8, 9, and 10−11)[20,21,23] and the numbers for the hydroxyl group (2.0−3.0 and 1.6−2.4)[18,21] and the ring oxygen (0.8).[21] The fluctuation of hydration around methyl α-D-Glc during the 20 ns simulations was examined by plotting the numbers of water molecules exhibiting hydrogen bonding to the α-GT rotamer (total), the hydroxyl group at C-4, and the ring oxygen (O-5) against the simulation time (Figure 4b). It is evident that the numbers of hydrated water molecules varied within the ranges of 6−14 (total), 0−4 (hydroxyl group at C-4), and 0−2 (ring oxygen). Similar changes in hydration numbers were also observed for the α-GG and α-TG rotamers (Figures S1b and S2b, Supporting Information). These results suggest that the configurations of hydroxyl groups and the sugar ring would extensively fluctuate accompanying the change of hydration to affect the VUV-ECD spectra of methyl α-D-Glc.

3.4. ECD Spectra of Simulated Structures of Methyl α-D-Glucopyranoside. Figure 5a shows the average ECD spectra calculated using the TDDFT method at the CAM-B3LYP/6-311++G** level for the 40 simulated structures of the α-GT, α-GG, and α-TG rotamers at 500 ps intervals (all of the theoretical spectra for each rotamer are shown in Figure 3S, Supporting Information). The hydrated water molecules around methyl α-D-Glc were ignored when calculating the ECD spectra. The ECD spectrum of α-GT exhibited a small positive peak around 185 nm and a negative peak around 165 nm, while the α-GG spectrum showed only a positive peak around 172 nm. The α-TG spectrum was characterized by a small positive peak around 180 nm and two negative peaks around 190 and 165 nm (with the 190 nm peak being very small). Figure 5b shows the ECD spectrum of methyl α-D-Glc, which was estimated by a linear combination of the α-GT, α-GG, and α-TG spectra based on their populations. Overall, this spectrum is similar to that observed experimentally, although the peak positions (175 and 165 nm) and intensities were not completely reproduced.

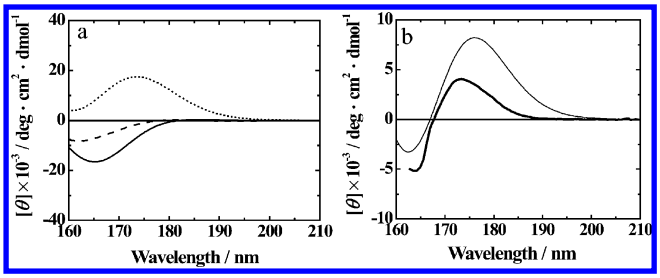

Figure 5. (a) Theoretical ECD spectra of methyl α-D-Glc calculated using the TDDFT method at the CAM-B3LYP/6-311++G** level for the α-GT (solid line), α-GG (dotted line), and α-TG (dashed line) rotamers. Each spectrum is the average of 40 spectra for the structures simulated at 500 ps intervals for 20 ns using AMBER software. (b) Theoretical (thin solid line) and experimental (thick solid line) ECD spectra of methyl α-D-Glc as estimated by a linear combination of the α-GT, α-GG, and α-TG spectra (as done for Figure 3).

The ECD spectra of the α-GT, α-GG, and α-TG rotamers cannot be measured experimentally because these rotamers are in equilibrium in an aqueous solution of methyl α-D-Glc. However, we have previously extracted these component spectra from the observed VUV-ECD spectra of D-glucose, D-mannose, and D-galactose using a nonlinear least-squares deconvolution analysis assuming a Gaussian distribution.[7] The obtained α-GT and α-GG spectra exhibited a negative peak around 167 nm and a positive peak around 170 nm, respectively.[7] Interestingly, the signs and positions of these two peaks are very close to those of the α-GT and α-GG spectra obtained by the simulation method employed in the present study (Figure 5a). Considering the similarity between the experimental and theoretical ECD spectra of methyl α-D-Glc (Figure 5b), the experimentally observed spectrum of methyl α-D-Glc can be considered to reflect a balance between the negative ECD of α-GT and the positive ECD of α-GG; the effects of the α-TG rotamer would be negligible because it constitutes only a few percent of the population in solution.[40] These results indicate that the fluctuations of configurations of methyl α-D-Glc obtained by MD simulations can be used to theoretically calculate reliable ECD spectra, leading to the assignment of ECD spectra and the characterization of solution structures of methyl α-D-Glc.

dx.doi.org/10.1021/jp306914s | J. Phys. Chem. A 2012, 116, 9996−10003

3.5. Assignments of VUV-ECD Spectrum of Methyl α-D-Glucopyranoside. Nelson and Johnson measured the VUV-ECD spectra of various methyl pyranosides and suggested that the first band (~185 nm) is due to the ring oxygen, the second (~175 nm) to the methoxy group, and the third (<165 nm) partly to the methoxy group.[5] On the other hand, based on the VUV-ECD spectra of various model compounds of D-glucopyranose and D-galactopyranose that differ only in the axial or equatorial configuration of the hydroxyl groups at C-2 and C-4, Bertucci et al. proposed that the two hydroxyl groups contribute greatly to the ECD spectra below 185 nm.[8] However, it would be difficult to estimate the effects of hydroxyl groups on the VUV-ECD spectra because the configuration of a hydroxyl group might affect not only its own electronic transitions but also those of the ring oxygen and other oxygen.

For further assignments of the ECD spectra of the α-GT, α-GG, and α-TG rotamers, the molecular orbitals and rotational strengths that participate in the electronic transitions of the hydroxyl group, the ring oxygen, and the methoxy oxygen were calculated using the TDDFT method at the CAM-B3LYP/6-311++G** level. The ECD in the wavelength region 180−170 nm was mainly assigned to the $n-\sigma^*$ transitions from the lone-pair orbital (n-orbital) to the σ^*-orbital of ring oxygen and methoxy oxygen, with only small contributions from hydroxyl groups. The effects of these chromophores extended to the wavelength region below 170 nm, although it was difficult to assign all of the transitions in the VUV region. These assignments were essentially consistent with the results of Nelson and Johnson[5] and Bertucci et al.[8]

3.6. Structural Differences among α-GT, α-GG, and α-TG Rotamers. As discussed above, the different ECD spectra of the α-GT, α-GG, and α-TG rotamers (Figure 5a) would be mainly attributable to changes in the rotational strengths of the ring oxygen (O-5) depending on the dihedral angle of the hydroxymethyl group of O-5−C-5−C-6−O-6 (+60, −60, or 180°). To clarify the steric configuration between the hydroxymethyl group and the ring oxygen, we plotted the dihedral angle of HO-6−O-6−C-6−C-5 against the distance between HO-6 and O-5 atoms in the three rotamers. As shown in Figure 6, the dihedral angles of HO-6−O-6−C-6−C-5 localized around −50 and 50° for the α-GT and α-GG rotamers, respectively, within the interatomic distance of 2.4 Å, where the hydrogen atom (HO-6) can form a hydrogen bond (as O-5−HO-6) to the ring oxygen (O-5) in both rotamers. This hydrogen bond was retained for about 15 ns of the total simulation time (20 ns) in both rotamers, indicating its high stability. On the other hand, the α-TG rotamer showed no converged dihedral angle within the interatomic distance of 2.4 Å, indicating that no hydrogen bond can be formed between HO-6 and O-5 atoms in the α-TG rotamer (Figure 6). However, the dihedral angle of HO-4−O-4−C-4−C-3 converged to about 180 or −180° within the distance of 2.4 Å between O-6 and HO-4 atoms and to about 50 or −50° within the distance of 2.4 Å between O-4 and HO-6 atoms (Figure S4, Supporting Information), indicating that two hydrogen bonds (i.e., O-6−HO-4 and O-4−HO-6) can be formed in the α-TG rotamer. Either of these two hydrogen bonds was retained for about 18 ns (10 ns for O-4−HO-6 and 8 ns for O-6−HO-4) of the total simulation time (20 ns). These hydrogen bonds would exert different perturbations on the chromophoric nonbonding electrons of the O-5 atom to produce the characteristic ECD spectra of the three rotamers.

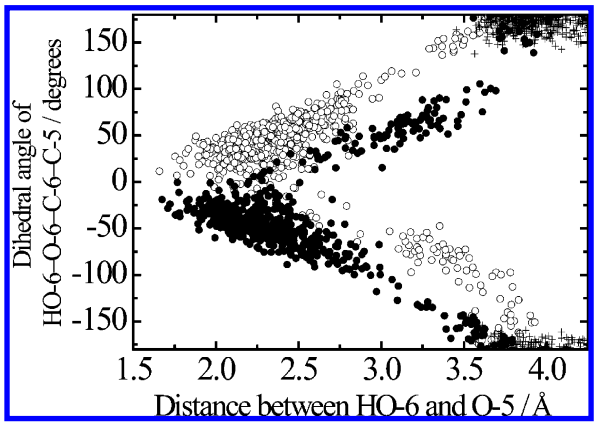

Figure 6. Plots of dihedral angles of HO-6−O-6−C-6−C-5 against the distance between HO-6 and O-5 atoms in the α-GT (filled circles), α-GG (open circles), and α-TG (plus signs) rotamers. The structure of each rotamer was simulated for 20 ns using AMBER software.

The different configurations of hydroxyl groups among the α-GT, α-GG, and α-TG rotamers were further examined by calculating the probabilities of the dihedral angles of HO-4−O-4−C-4−C-3, HO-3−O-3−C-3−C-2, and HO-2−O-2−C-2−C-1 at 10° intervals for the 20 ns simulation. As shown in Figure 7, these dihedral angles of the three rotamers distributed with a high probability around 60, 180, and 300°, which is similar to the results of Simmerling et al.[16] The α-GT and α-GG rotamers show very similar probability distributions for the dihedral angles of HO-4−O-4−C-4−C-3, HO-3−O-3−C-3−C-2, and HO-2−O-2−C-2−C-1. However, the distribution of the dihedral angle of HO-4−O-4−C-4−C-3 is very different for the α-TG rotamer than for the other two rotamers, which is due to the hydroxyl group at C-4 forming stable hydrogen bonds with the hydroxyl group at C-6. Since the probabilities of other configurations involving the methoxy group and sugar ring were similar among the three rotamers (data not shown), the differences in the ECD spectra of the α-GT and α-GG rotamers (Figure 5a) would be mainly due to the different configurations of the hydroxymethyl group at C-5. However, the ECD spectra of α-TG would be different from the others due to the different configurations of the hydroxyl group at C-4 in addition to the hydroxymethyl group at C-5. The speculative steric configurations around the ring oxygen of the α-GT, α-GG, and α-TG rotamers based on these results are shown in Figure 8. The α-GT and α-GG rotamers exhibit different geometries for the orientation of the hydrogen bond between O-5 and HO-6 atoms while keeping symmetrical configurations around the ring oxygen (O-5). On the other hand, the α-TG rotamer can form two types of hydrogen bonds: O-6−HO-4 and O-4−HO-6. These differences in hydrogen bonds would be responsible for the characteristic ECD spectra of the α-GT, α-GG, and α-TG rotamers. Thus, the structural differences between these three rotamers provide new information on the principle of pairwise relationships between the configurations of chromophores and the VUV-ECD spectra of monosaccharides.

4. CONCLUSIONS

The present study is the first to calculate the VUV-ECD spectrum of methyl α-D-Glc in aqueous solution using the TDDFT method. Despite some limitations, the theoretical ECD spectrum for the structures simulated using AMBER software successfully reproduced the peak intensities and

dx.doi.org/10.1021/jp306914s | J. Phys. Chem. A 2012, 116, 9996−10003

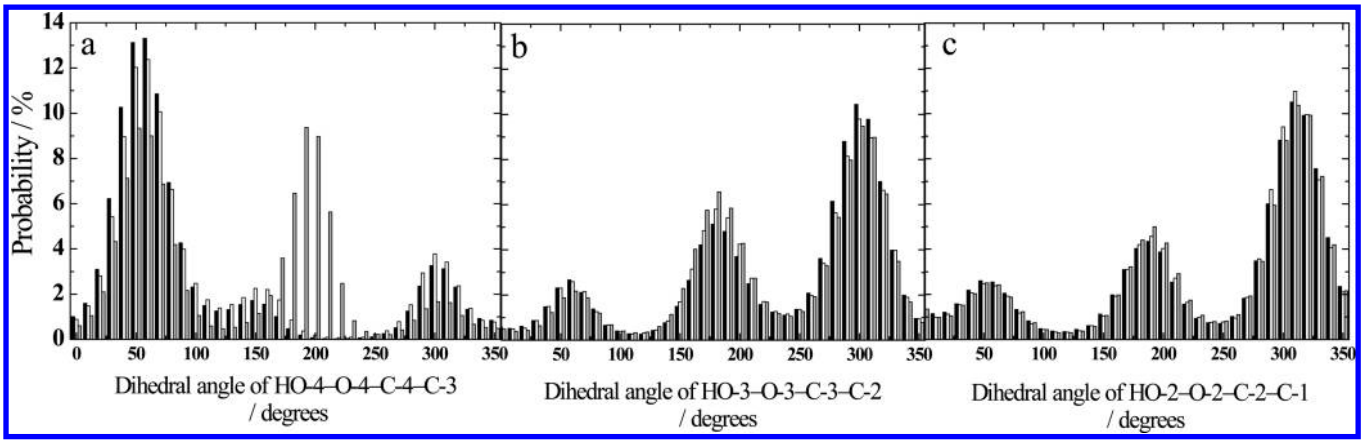

Figure 7. Distributions of probabilities of dihedral angles of (a) HO-4−O-4−C-4−C-3, (b) HO-3−O-3−C-3−C-2, and (c) HO-2−O-2−C-2−C-1 in the α-GT (black), α-GG (white), and α-TG (gray) rotamers. The structure of each rotamer was simulated for 20 ns using AMBER software.

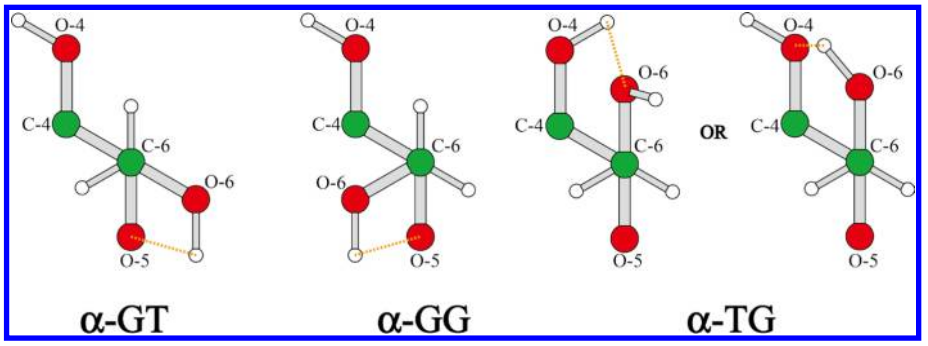

Figure 8. Speculative steric configurations around the ring oxygen and the hydroxymethyl group of the α-GT, α-GG, and α-TG rotamers in aqueous solution. Oxygen, hydrogen, and carbon atoms are colored red, white, and green, respectively. Yellow dotted lines indicate hydrogen bonds. The view in each figure is looking down the bond from C-6 to C-5.

positions of the experimentally observed spectrum, and also revealed the characteristic conformations and VUV-ECD spectra of the α-GT, α-GG, and α-TG rotamers, which are not observable experimentally. These results demonstrate that combining VUV-ECD spectroscopy, MD, and TDDFT is very useful for analyses of the solution structures of D-glucose and other saccharides. Further accumulation of VUV-ECD spectra and theoretical calculations of saccharides would open new fields in the molecular sciences of glycoconjugates.

■ ASSOCIATED CONTENT

Ⓢ Supporting Information

Plots of the dihedral angles of HO-4−O-4−C-4−C-3 in the α-GG and α-TG rotamers against the simulation time (Figures S1a and S2a), plots of the numbers of hydrated water molecules (total, hydroxyl group at C-4, and O-5) in the α-GG and α-TG rotamers against the simulation time (Figures S1b and S2b), all theoretical ECD spectra of simulated α-GT, α-GG, and α-TG rotamers (Figure S3), plots of the dihedral angle of HO-4−O-4−C-4−C-3 against the distances between HO-4 and O-6 atoms and between O-4 and HO-6 atoms for the α-TG rotamer (Figure S4), and a full list of the authors of refs 31 and 32. This material is available free of charge via the Internet at http://pubs.acs.org.

■ AUTHOR INFORMATION

Corresponding Author

*E-mail: pika@hiroshima-u.ac.jp. Phone: +81 82 424 6293. Fax: +81 82 424 6294.

Notes

The authors declare no competing financial interest.

■ ACKNOWLEDGMENTS

This work was supported by a JSPS Research Fellowship for Young Scientists (K.M.) (nos. 19001913 and 23687020) and a Grant-in-Aid for Scientific Research (no. 20550153) from the Ministry of Education, Science, Sports, and Culture of Japan (K.G.).

■ REFERENCES

(1) Johnson, W. C. *Adv. Carbohydr. Chem. Biochem.* **1987**, *45*, 73−124.
(2) Berova, N.; Nakanishi, K.; Woody, R. W. *Circular Dichroism: Principles and Applications*, 2nd ed.; John Wiley & Sons: New York, 2000.
(3) Fasman, G. D. *Circular Dichroism and the Conformational Analysis of Biomolecules*; Plenum Press: New York, 1996.
(4) Nelson, R. G.; Johnson, W. C. *J. Am. Chem. Soc.* **1972**, *94*, 3343−3345.
(5) Nelson, R. G.; Johnson, W. C. *J. Am. Chem. Soc.* **1976**, *98*, 4296−4301.
(6) Arndt, E. R.; Stevens, E. S. *J. Am. Chem. Soc.* **1993**, *115*, 7849−7853.
(7) Matsuo, K.; Gekko, K. *Carbohydr. Res.* **2004**, *339*, 591−597.
(8) Bertucci, C.; Salvadori, P.; Giampaolo, Z.; Pini, D.; Johnson, W. C., Jr. *Carbohydr. Chem.* **1986**, *149*, 299−307.
(9) Ojima, N.; Sakai, K.; Matsuo, K.; Matsui, T.; Fukazawa, T.; Namatame, H.; Taniguchi, M.; Gekko, K. *Chem. Lett.* **2001**, *30*, 522−523.

(10) Matsuo, K.; Sakai, K.; Matsushima, Y.; Fukuyama, T.; Gekko, K. *Anal. Sci.* **2003**, *19*, 129−132.
(11) Matsuo, K.; Namatame, H.; Taniguchi, M.; Gekko, K. *Biosci., Biotechnol., Biochem.* **2009**, *73*, 557−561.
(12) Appell, M.; Strati, G.; Willett, J. L.; Momany, F. A. *Carbohydr. Res.* **2004**, *339*, 537−551.
(13) Momany, F. A.; Appell, M.; Strati, G.; Willett, J. L. *Carbohydr. Res.* **2004**, *339*, 553−567.
(14) Momany, F. A.; Appell, M.; Willetta, J. L.; Bosmac, W. B. *Carbohydr. Res.* **2005**, *340*, 1638−1655.
(15) Schnupf, U.; Willett, J. L.; Momany, F. A. *Carbohydr. Res.* **2010**, *345*, 503−511.
(16) Simmerling, C.; Fox, T.; Kollman, P. A. *J. Am. Chem. Soc.* **1998**, *120*, 5771−5782.
(17) Kirschner, K. N.; Woods, R. J. *Proc. Natl. Acad. Sci. U.S.A.* **2001**, *98*, 10541−10545.
(18) Suzuki, T.; Kawashima, H.; Sota, T. *J. Phys. Chem. B* **2006**, *110*, 2405−2418.
(19) Suzuki, T. *Phys. Chem. Chem. Phys.* **2008**, *10*, 96−105.
(20) Caffarena, E. R.; Grigera, J. R. *Carbohydr. Res.* **1999**, *315*, 63−69.
(21) Molteni, C.; Parrinello, M. *J. Am. Chem. Soc.* **1998**, *120*, 2168−2171.
(22) Sakurai, M.; Murata, H.; Inoue, Y.; Hino, A.; Kobayashi, S. *Bull. Chem. Soc. Jpn.* **1997**, *70*, 847−858.
(23) Lee, S. L.; Debenedetti, P. G.; Errington, J. R. *J. Chem. Phys.* **2005**, *122*, 204511−204519.
(24) Fukuyama, T.; Matsuo, K.; Gekko, K. *J. Phys. Chem. A* **2005**, *109*, 6928−6933.
(25) Fukuyama, T.; Matsuo, K.; Gekko, K. *Chirality* **2011**, *23*, E52−58.
(26) Šebek, J.; Gyurcsik, B.; Šebestik, J.; Kejík, Z.; Bednárová, L.; Bour, P. *J. Phys. Chem. A* **2007**, *111*, 2750−2760.
(27) Nielsen, L. M.; Holm, A. I. S.; Varsano, D.; Kadhane, U.; Hoffmann, S. V.; Di Felice, R.; Rubio, A.; Nielsen, S. B. *J. Phys. Chem. B* **2009**, *113*, 9614−9619.
(28) Pérez, S.; Delage, M.-M. *Carbohydr. Res.* **1991**, *212*, 253−259.
(29) Yanai, T.; Tew, D. P.; Handy, N. C. A. *Chem. Phys. Lett.* **2004**, *393*, 51−57.
(30) Racaud, A.; Allouche, A. R.; Antoine, R.; Lemoine, J.; Dugourd, P. *J. Mol. Struct.: THEOCHEM* **2010**, *960*, 51−56.
(31) Frisch, M. J.; Trucks, G. W.; Schlegel, H. B.; Scuseria, G. E.; Robb, M. A.; Cheeseman, J. R.; Montgomery, J. A., Jr.; Vreven, J., T.; Kudin, K. N.; Burant, J. C.; et al. *Gaussian 09*, revision A.03; Gaussian, Inc.: Wallingford, CT, 2009.
(32) Case, D. A.; Darden, T. A.; Cheatham, T. E.; Simmerling, C. L.; Wang, J.; Duke, R. E.; Luo, R.; Walker, R. C.; Zhang, W.; Merz, K. M.; et al. *AMBER 11*; University of California: San Francisco, CA, 2010.
(33) Jorgensen, W. L.; Jenson, C. *J. Comput. Chem.* **1998**, *19*, 1179−1186.
(34) Kirschner, K. N.; Yongye, A. B.; Tschampel, S. M.; Gonzalez-Outeiriño, J.; Daniels, C. R.; Foley, B. L.; Woods, R. *J. Comput. Chem.* **2007**, *29*, 622−655.
(35) Berendsen, H. J. C.; Postma, J. P. M.; van Gunsteren, W. F.; DiNola, A.; Haak, J. R. *J. Chem. Phys.* **1984**, *81*, 3684−3690.
(36) Darden, T.; York, D.; Pedersen, L. *J. Chem. Phys.* **1993**, *98*, 10089−10092.
(37) Ryckaert, J. P.; Ciccotti, G.; Berendsen, H. J. C. *J. Comput.Phys.* **1977**, *23*, 327−341.
(38) Cheeseman, J. R.; Shaik, M. S.; Popelier, P. L. A.; Blanch, E. W. *J. Am. Chem. Soc.* **2011**, *133*, 4991−4997.
(39) Miertus, S.; Scrocco, E.; Tomasi, J. *Chem. Phys.* **1981**, *55*, 117−129.
(40) Nishida, Y.; Hori, H.; Ohrui, H.; Megro, H. *J. Carbohydr. Chem.* **1988**, *7*, 239−250.
(41) Hollenberg, J. L.; Ifft, J. B. *J. Phys. Chem.* **1982**, *86*, 1938−1941.
(42) Bonner, O. D.; Woolsey, G. B. *J. Phys. Chem.* **1968**, *72*, 899−905.
(43) Galema, S. A.; Høiland, H. *J. Phys. Chem.* **1991**, *95*, 5321−5326.
(44) Nomura, H.; Kobe, S.; Matsuomoto, K.; Miyahara, Y. In *Studies in Physical and Theoretical Chemistry*; Tanaka, N., Ohtaki, H., Tamamushi, R., Eds.; Elsevier: Amsterdam, The Netherlands, 1982; Vol. *27*, p 151.
(45) Tait, M. J.; Suggett, A.; Franks, F.; Ablett, S.; Quickenden, P. A. *J. Solution Chem.* **1972**, *1*, 131−151.